High Reusability of NiAl LDH/Biochar Composite in the Removal Methylene Blue from Aqueous Solution

Aldes Lesbani[1,2*], Neza Rahayu Palapa[1], Rabellia Juladika Sayeri[2], Tarmizi Taher[3], and Nurlisa Hidayati[4]

[1]*Graduate School of Mathematics and Natural Sciences, Faculty of Mathematics and Natural Sciences, Universitas Sriwijaya, Jl. Palembang Prabumulih Km. 32, Ogan Ilir 30662, Indonesia*

[2]*Research Center of Inorganic Materials and Coordination Complexes, Faculty of Mathematics and Natural Sciences, Universitas Sriwijaya, Jl. Palembang Prabumulih Km. 32, Ogan Ilir 30662, Indonesia*

[3]*Department of Environmental Engineering, Institut Teknologi Sumatera, Jl. Terusan Ryacudu, Way Hui, Kecamatan Jati Agung, Lampung Selatan 35365, Indonesia*

[4]*Department of Chemistry, Faculty of Mathematics and Natural Sciences, Universitas Sriwijaya, Jl. Palembang Prabumulih Km. 32, Ogan Ilir 30662, Indonesia*

* ***Corresponding author:***

email: aldeslesbani@pps.unsri.ac.id

Received: June 16, 2020
Accepted: January 4, 2021

DOI: 10.22146/ijc.56955

Abstract: *Ni/Al layered double hydroxide was used as a starting material for composite formation with biochar as a matrix. The materials were characterized using X-ray, FTIR, nitrogen adsorption-desorption, thermal, and morphology analyses. The NiAl LDH/Biochar material is then used as an adsorbent of methylene blue from an aqueous solution. The factor that was influencing adsorption such as pH, time, methylene blue concentration, and temperature adsorption was studied systematically. The regeneration of adsorbent was performed to know the stability of NiAl LDH/Biochar under several cycle adsorption processes. The results showed that NiAl LDH/Biochar has a specific diffraction peak at 11.63° and 22.30°. NiAl LDH/Biochar has more than ten-fold surface area properties (438,942 m^2/g) than biochar (50.936 m^2/g), and Ni/Al layered double hydroxide (92.682 m^2/g). The methylene blue adsorption on NiAl LDH/Biochar follows a pseudo-second-order kinetic adsorption model and classify as physical adsorption. The high reusability properties were found for NiAl LDH/Biochar, which was largely different from biochar and Ni/Al layered double hydroxide.*

Keywords: *Ni/Al; layered double hydroxide; biochar; composite; methylene blue; adsorption; reusability*

■ INTRODUCTION

The presence of hazardous dyes in industrial activities is a severe problem for humans and the ecology system [1]. These dyes are toxic, carcinogenic, and mutagenic, thus cause human and environmental health. The dyes are produced from industrial activities such as cosmetics, painting, textile, leather, food, and also drug industries [2-4]. The dyes are challenging to degrade since they are stable structures under oxidation and light [5]. One of the toxic dyes is methylene blue, a methylthioninium chloride compound and classifies as a cationic dye [6]. The structure of methylene blue is shown in Fig. 1. Thus, the removal of methylene blue from wastewater is crucial. Some methods are available to remove methylene blue from an aqueous solution, such as purification, membrane separation, and adsorption [7-9].

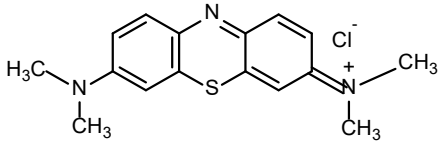

Fig 1. Chemical structure of methylene blue

Among these methods, adsorption is an appropriate method to remove methylene blue from the aqueous solution. This method was easy to do, simple way, low-cost operation, and fast process [10]. On the other hand, the effectivity of adsorbent in the adsorption process is one factor in getting high adsorption capacity and stability of the material. Numerous adsorbents have been applied to remove methylene blue from an aqueous solution, such as zeolite, bentonite, carbon nanotube, biomass, activated carbon, chitosan, and also layered double hydroxide [11-13].

Layered double hydroxide (LDH) is an inorganic material that has the general formula $[M^{2+}_{1-x}M^{3+}_{x}(OH)_2] + xA_x^{-n}mH_2O$, where M^{2+} is a divalent metal ion, M^{3+} is a trivalent metal ion, A_x^{-n} is an anion with n valent state, and water of crystallization [14-15]. LDH consists of an anion on the interlayer distance, which can be exchangeable to other anions to get unique properties of LDH. The common anion in LDH is nitrate, sulfate, hydroxide, chloride, and carbonate [16-18]. The total charge of LDH is positively due to neutralizing negative charge from anion on interlayer space. LDH has well-known as an adsorbent of dyes due to its high adsorption capacity and high surface area properties.

On the other hand, the use of LDH several times the regeneration process is ineffective due to sprayed and exfoliated LDH structure [19]. Thus modification of LDH for reuse adsorbent aim should be conducted, such as the formation of the composite using matrix/support materials which can reduce the particle size of LDH to be facile for reuse adsorbent. One of the promising materials as a matrix for LDH is biochar. Biochar is an organic compound from the pyrolysis of biomass under high temperature [20]. The use of biochar for many applications is reported, such as water treatment, soil improvement materials, and also pharmaceutical applications [21-22]. The composite of LDH-biochar as an adsorbent of many organic and inorganic pollutants has been reported in many publications.

MgAl and Mg/Fe-biochar were prepared as adsorbents of phosphate [23]. Phosphate was also successfully removed from an aqueous solution using Mg/Al LDH-biochar [24]. Biochar from date palm was used as a matrix for the composite of MgAl LDH-biochar. This biochar has an adsorption capacity of 302.75 mg/g at 100 mg/L in 180 min adsorption time [25]. LDH Mg/Al-biochar has been prepared to form a composite as an adsorbent of methylene blue. This adsorbent can achieve adsorption capacity until 406.47 mg/g [9]. Lins et al. [26] introducing liquid phase co-precipitation of Mg-Al LDH on a biochar matrix for enhanced phosphate adsorption. Wang et al. [27] reporting high arsenic adsorption onto Ni–Fe LDH-biochar composite. Despite different biochars used, these studies, in general, suggest that selective adsorption of anionic pollutants depends on the type of LDHs used, and the adsorption mechanisms are linked to interlayer spacing and electrical properties of LDHs. All these studies showed that LDH is commonly used to prepare composite using biochar as a matrix.

This study aims to use LDH based nickel-aluminum as a starting material to form a composite with biochar as an adsorbent of methylene blue. Formation of Ni/Al LDH/biochar was prepared by mixing the co-precipitation method. The materials were characterized using X-ray, FTIR, BET, thermal, and photo SEM-EDX analyses. The adsorption was studied through the effect of pH medium, adsorption time, initial concentration of methylene blue, and temperature adsorption. The performance of the adsorbent was investigated through reusability adsorbent several times. Prior to these processes, desorption is conducted to know the suitable solvent to desorb methylene blue on the solid adsorbent.

■ EXPERIMENTAL SECTION

Chemicals and Instrumentation

Chemicals used in this research were nickel(II) nitrate, aluminum(III) nitrate, sodium hydroxide, and methylene blue. These chemical reagents were used directly from Merck and Sigma-Aldrich without further purification. Biochar based on Indonesian rice husk was obtained from Bukata Organic, Java Island. Water was obtained from Research Center of Inorganic Materials and Complexes FMIPA Universitas Sriwijaya using Purite® water ion exchange purification system.

Characterization of the material was performed using X-ray Rigaku Miniflex-6000. The material was analyzed in the range 5–80° with scan speed 1°/min. FTIR spectrum was obtained from FTIR Shimadzu Prestige-21. Materials were mixed with KBr to form a pellet and were scanned at wavenumber 400–4000 cm^{-1}. Nitrogen adsorption-desorption analysis was conducted using ASAP Micrometric at 77 K. Sample was degassed under liquid nitrogen several times prior to analysis. The thermal stability of the material was measured using TG-DTA Shimadzu under atmospheric nitrogen. The temperature analysis was at room temperature to 800 °C. Material photos were obtained using SEM-EDX Quanta-650 Oxford Instrument. The concentration of methylene blue was analyzed using UV-Visible spectrophotometer BIO-Base BK-UV 1800 PC at wavelength 664 nm.

Procedure

Synthesis of Ni/Al LDH

Synthesis of Ni/Al LDH was conducted using the co-precipitation method at pH 10 [28]. Nickel(II) nitrate and aluminum(III) nitrate with equal volume and concentration ratio (3:1) were mixed and stirred at room temperature. Sodium carbonate (0.3 M) was added with equal volume slowly and sodium hydroxide to achieve pH 10. The reaction mixture was kept at 80 °C for 18 h. The solid material was obtained and washed with water, and dried at 110 °C.

Synthesis of composite Ni/Al LDH-biochar

Synthesis of NiAl LDH/Biochar was conducted by mixing the co-precipitation method. The solution of nickel(II) nitrate 0.3 M and aluminum(III) nitrate 0.1 M with equal volume was mixed for 60 min. Biochar (3 g) was added to the reaction mixture following by the addition of sodium hydroxide (2 M). The pH mixture was adjusted to 10 by adding sodium hydroxide. The reaction was kept for 72 h with constant stirring. The solid material was obtained and washed several times with water, and dried at 110 °C for several days.

Adsorption process

Adsorption was studied by variation of pH solution, adsorption time, initial concentration, and adsorption temperature using 0.1 g of NiAl LDH/Biochar and starting materials as control. The adsorption was conducted using a batch small reactor system equipped with shaking apparatus control. The variation pH solution was 2–10. Adsorption time was conducted at 5–200 min. Adsorption temperature was carried out at 30, 40, 50, and 60 °C using an initial concentration of methylene blue from 5–20 mg/L for NiAl LDH as adsorbent, 5–40 mg/L for biochar, and 5–60 mg/L for NiAl LDH/Biochar. All filtrate of methylene blue was analyzed using UV-Visible at wavelength 664 nm.

Desorption and regeneration

Desorption of methylene blue after the adsorption process was conducted using several solvents such as ethanol, acetone, diethyl ether, water, hydrochloric acid, and sodium hydroxide. The solvent has been classified as organic and inorganic solvents. The filtrate from the desorption process was measured using UV-Vis at 664 nm.

Prior regeneration process, the adsorbent was desorbed using maximum desorption solvent followed by washed using water several times, dried at 110 °C overnight, and ready to use. The cycle of adsorption was conducted three times the cycle for adsorption of methylene blue using a similar adsorbent.

■ RESULTS AND DISCUSSION

The results of XRD pattern of NiAl LDH/Biochar, biochar, and Ni/Al LDH were shown in Fig. 2. Fig. 2(a) showed Ni/Al LDH has peak at 11.63° (003); 23.00° (006); 35.16° (012); 39.56° (015); 47.4° (018) and 61.59° (110). The formation of a well-layered structure of Ni/Al was identified at 11.63 (003) and 61.59 (110) [29]. These results are appropriate with Tao et al. (2019) where the crystallinity of Ni/Al LDH was high [30]. Fig. 2(b) shows the diffraction of biochar. Biochar is an organic compound; thus, the diffraction peak is board due to the high organic content on the material. The diffraction peak at 22.30° (002) for biochar was characteristic of organic content, especially carbon [31-32]. Fig. 2(c) shows the NiAl LDH/Biochar based Ni/Al LDH and biochar. The diffraction peak of NiAl LDH/Biochar is a little broad, with several peaks were identified at 11.63° and 22.30°. These two peaks are Ni/Al LDH and biochar

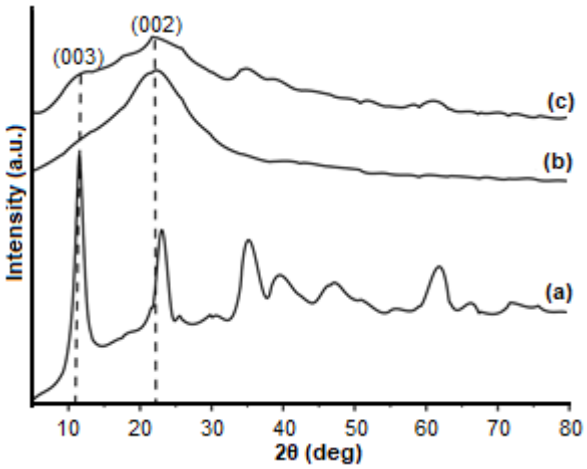

Fig 2. X-ray diffraction of Ni/Al LDH (a), biochar (b), and NiAl LDH/Biochar (c)

characterized; thus, NiAl LDH/Biochar consists of LDH and biochar.

FTIR spectrum of materials was presented in Fig. 3. Fig. 3(a) shows the IR spectrum of Ni/Al LDH. The peak vibration was appeared at 3664 cm^{-1} (υ O–H stretching), 1630 cm^{-1} (υ O–H bending), 1381 cm^{-1} (υ N–O nitrate), 748 cm^{-1} (υ Al–O, trivalent metal), and 563 cm^{-1} (υ Ni–O, divalent metal) [24]. Fig. 3(b) shows the FTIR spectrum of biochar. There are several peaks identified at wavenumber 3448 cm^{-1}, 2924 cm^{-1}, 2854 cm^{-1}, 2368 cm^{-1}, 2337 cm^{-1}, 1620 cm^{-1}, and 1130 cm^{-1}. All these vibrations were identified in the fingerprint area and consist of an organic vibration component [33]. Fig. 3(c) shows the FTIR spectrum of NiAl LDH/Biochar. The peaks are found at 3441 cm^{-1}, 2931 cm^{-1}, 2368 cm^{-1}, 2283 cm^{-1}, 1627 cm^{-1}, 1381 cm^{-1}, 1049 cm^{-1}, and 578 cm^{-1}. All these vibrations contain vibrations of Ni/Al LDH and biochar. Thus, NiAl LDH/Biochar in this research is based on two components.

The nitrogen adsorption-desorption analysis data of Ni/Al LDH, biochar, and NiAl LDH/Biochar was shown in Fig. 4. The isotherm in Fig. 4 shows a hysteresis loop where the adsorption curve has a different type from the desorption step. The NiAl LDH/Biochar has a type II isotherm model, and the material has a mesoporous class with contains a larger pore than the microporous type [34]. The isotherm data in Fig. 4 was then used to obtain surface area, pore-volume, and pore diameter, as shown in Table 1.

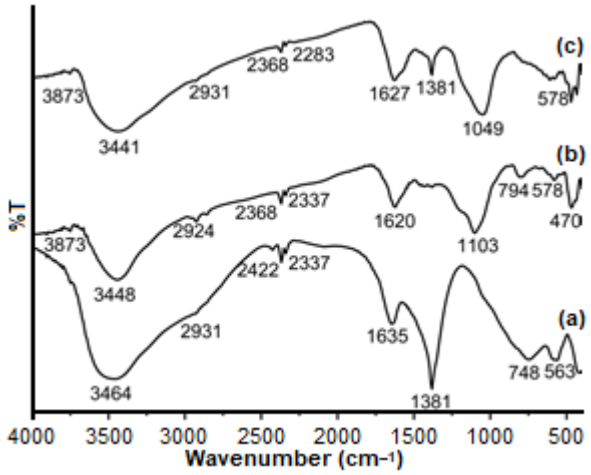

Fig 3. FTIR spectrum of Ni/Al LDH (a), biochar (b), and NiAl LDH/Biochar (c)

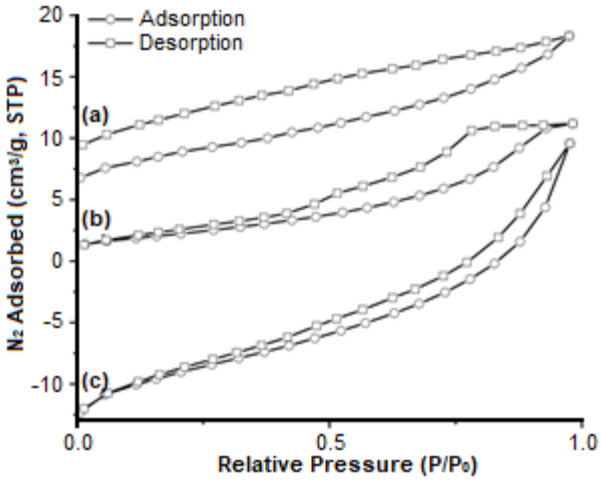

Fig 4. Nitrogen adsorption-desorption profile of Ni/Al LDH (a), biochar (b), and NiAl LDH/Biochar (c)

Table 1. BET surface area analysis

Materials	Surface area (m^2/g)	Pore volume (cm^3/g)	Pore diameter (nm)
Ni/Al LDH	92.683	0.001	13.206
Biochar	50.936	0.002	12.088
NiAl LDH/Biochar	438.942	0.002	12.301

Table 1 shows NiAl LDH/Biochar has large surface area properties than Ni/Al LDH and biochar. The NiAl LDH/Biochar has a surface area of 438.942 m^2/g and almost ten-fold higher than starting materials. These phenomena are probably due to the biochar as matrix-assisted to reduce the size and agglomeration of LDH [23].

The TG-DTA pattern of the material was presented in Fig. 5. Ni/Al LDH has two endothermic peaks at 90 °C and 310 °C, which is assigned as water loss and nitrate on interlayer LDH decomposition. On the other hand, the DTA profile of biochar contains not only an endothermic peak but also an exothermic peak. The endothermic peak was found at 95 °C due to the loss of water of crystallization [11]. The exothermic peak was found at 500 °C because of the oxidation of organic compounds on biochar [35]. The TG-DTA pattern of NiAl LDH/Biochar was shown in Fig. 5(c) and contained one endothermic peak at 95 °C and two exothermic peaks at 430 °C and 500 °C. The exothermic peaks are the LDH decomposition peak, and the endothermic peak is the oxidation of organic biochar.

The surface material photos were presented in Fig. 6. The layer structure of Ni/Al was seen in Fig. 6(a) with the agglomeration process. The biochar, as seen in Fig. 6(b) has an irregular pore. The NiAl LDH/Biochar shown in Fig. 6(c) has small particle distribution than

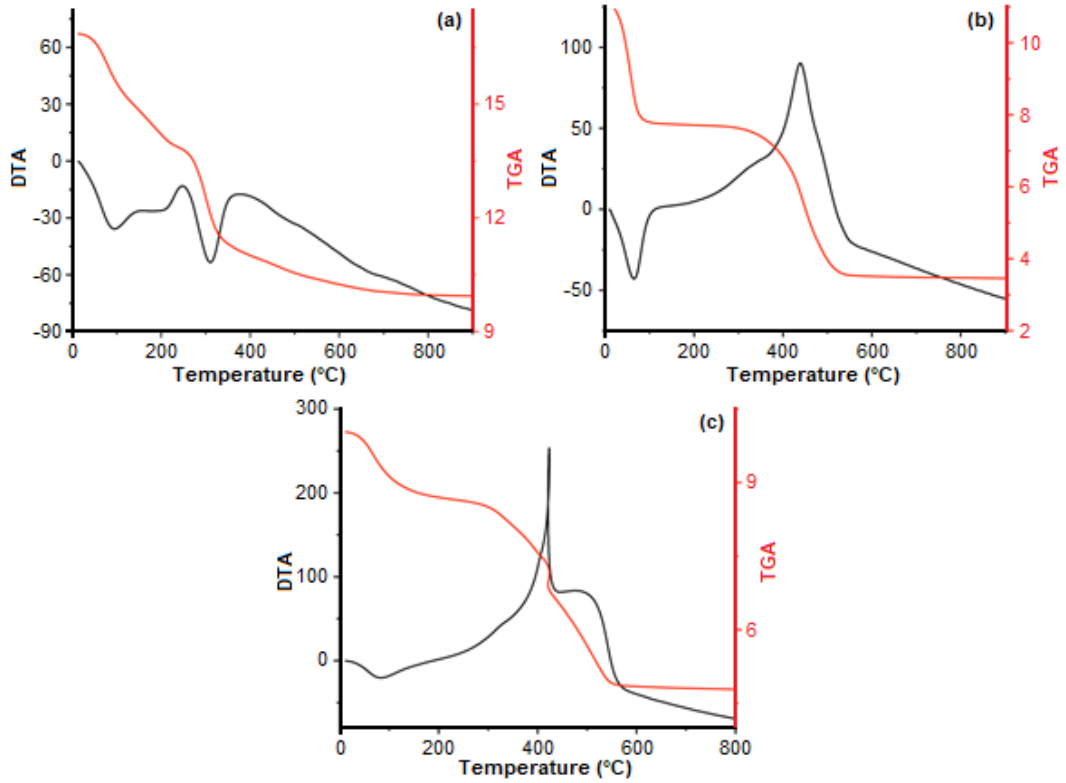

Fig 5. TG-DTA profile of Ni/Al LDH (a), biochar (b), and NiAl LDH/Biochar (c)

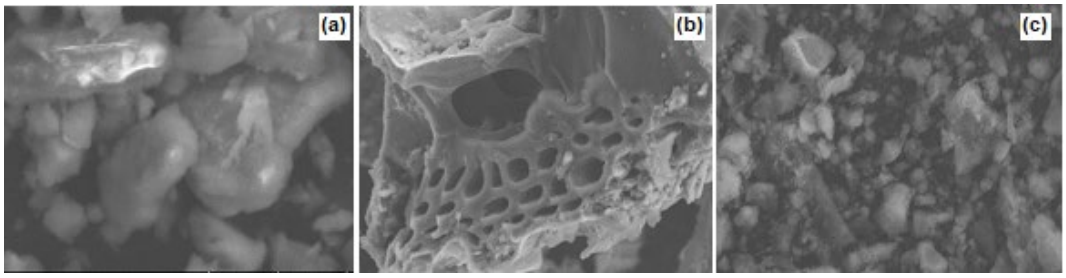

Fig 6. Surface photo of materials

Ni/Al LDH with minor agglomeration. These photos in Fig. 6(c) are related to a high surface area of NiAl LDH/Biochar in this research.

The composition of materials analysis using EDX was shown in Table 2. The main composition of LDH was nickel, aluminum, oxygen, and nitrogen. Nitrogen is higher because nitrate ion was located on the interlayer scape of LDH. Biochar has high carbon content (58.3%). The NiAl LDH/Biochar contains all elements of starting materials except carbon because carbon is associated with oxygen in the agglomeration process, and the percentage of oxygen will be higher than starting materials.

The effect of the pH medium of methylene blue adsorption on Ni/Al LDH, biochar, and NiAl LDH/Biochar is shown in Fig. 7. The optimum pH for NiAl LDH/Biochar, biochar, and NiAl LDH was 4, 4, and 3. All adsorbents have methylene blue adsorption at acid medium. The solution of methylene blue has a pH range of 3.0–4.3, the optimum pH adsorption using NiAl LDH/Biochar, biochar, and Ni/Al LDH is inside the natural range of methylene blue, for further adsorption was conducted at this optimum pH.

Fig. 8 shows the effect of adsorption time and fitting with kinetic pseudo-first-order (PF-O) and pseudo-second-order (PS-O). The amount of methylene blue adsorbed on NiAl LDH/Biochar, biochar, and Ni/Al LDH was gradually increased by increasing adsorption time until optimum. The amount of methylene blue stable on the adsorbent. The optimum adsorption time for NiAl LDH/Biochar, biochar, and Ni/Al LDH is started from 150 min, as shown in the black circle symbol. These data then were applied to obtain PF-O and PS-O using the equation as following [36]:

PF-O:

$$\log(q_e - q_t) = \log q_e - \left(\frac{k_1}{2.303}\right)t \quad (1)$$

where: q_e is adsorption capacity at the equilibrium (mg g^{-1}); q_t is adsorption capacity at t min (mg g^{-1}); t is adsorption time (min), and k_1 is kinetic adsorption rate at PF-O (min^{-1}).

PS-O:

$$\frac{t}{q_t} = \frac{1}{k_2 q_e^{\,2}} + \frac{1}{q_e}t \quad (2)$$

where q_e is adsorption capacity at the equilibrium (mg g^{-1}); q_t is adsorption capacity at t min (mg g^{-1}); t is adsorption time (min), and k_2 is adsorption rate at PS-O (g mg^{-1} min^{-1}). The PF-O and PS-O results are shown in Table 3.

The data in Table 3 showed that the R^2 value for NiAl LDH/Biochar and biochar is closed to one for PS-O. On the other hand, Ni/Al LDH has R^2 closed to one

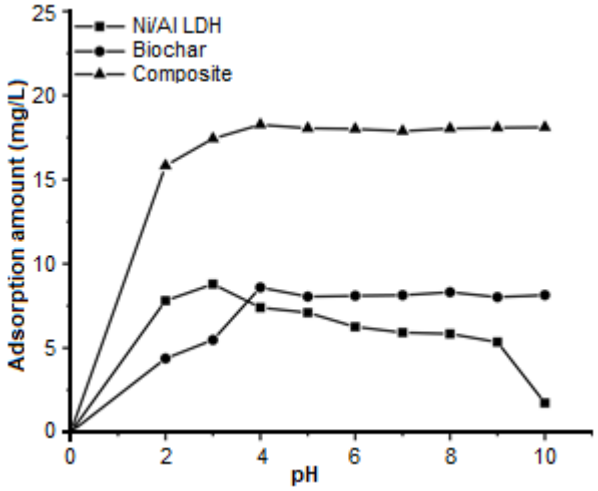

Fig 7. The pH adsorption effect of methylene blue on Ni/Al LDH, biochar, and NiAl LDH/Biochar

Table 2. Analysis composition of materials by EDX

Ni/Al LDH		Biochar		NiAl LDH/Biochar	
Element	(%)	Element	(%)	Element	(%)
Ni	88.3	C	58.3	Ni	14.6
Al	1.3	O	27.3	Al	3.3
O	1.4	Si	11.0	N	1.3
N	9.1	Al	3.3	O	55.6
				Si	25.2

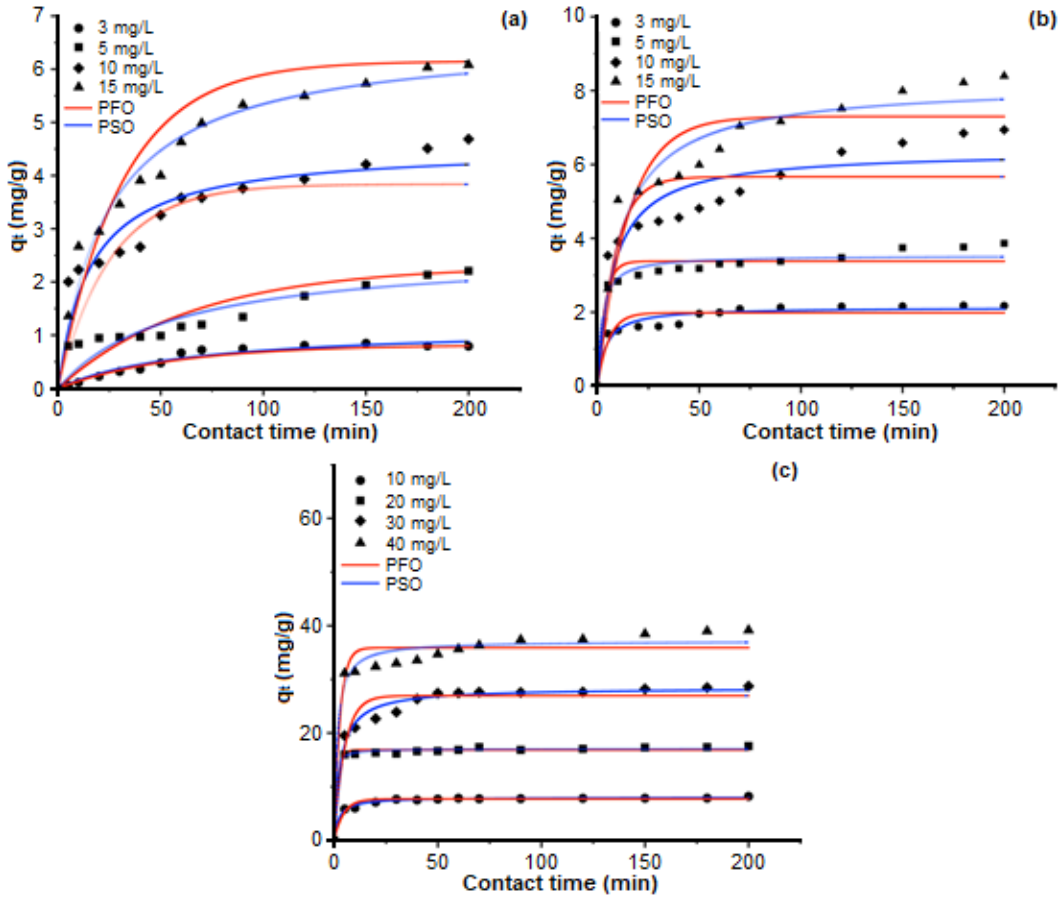

Fig 8. Kinetic adsorption of methylene blue on Ni/Al LDH (a), biochar (b), and NiAl LDH/Biochar (c)

Table 3. Kinetic parameter of pseudo first-order and second-order

Kinetic Models	Parameter	3 mg/L	5 mg/L	10 mg/L	15 mg/L
		Ni/Al LDH			
Pseudo first order	q_e exp (mg/g)	0.396	1.183	2.343	3.258
	q_e calc (mg/g)	1.924	1.073	1.603	2.922
	k_1 (min^{-1})	0.033	0.012	0.014	0.022
	R^2	0.921	0.921	0.955	0.939
Pseudo second order	q_e exp (mg/g)	0.396	1.183	2.343	3.258
	q_e calc (mg/g)	0.620	10.417	7.299	4.484
	k_2 (g/mg min)	0.020	0.004	0.004	0.014
	R^2	0.900	0.964	0.920	0.917
		Biochar			
Pseudo first Order	q_e exp (mg/g)	1.085	1.932	3.469	4.198
	q_e calc (mg/g)	1.554	1.312	2.582	2.843
	k_1 (min^{-1})	0.035	0.015	0.020	0.018
	R^2	0.961	0.857	0.929	0.961
Pseudo second order	q_e exp (mg/g)	1.085	1.932	3.469	4.198
	q_e calc (mg/g)	1.133	1.951	7.633	2.222
	k_2 (g/mg min)	0.114	0.062	0.006	0.104
	R^2	0.997	0.995	0.971	0.942

Table 3. Kinetic parameter of pseudo first-order and second-order (*Continued*)

Kinetic Models	Parameter	3 mg/L	5 mg/L	10 mg/L	15 mg/L
NiAl LDH/Biochar					
Pseudo first order	q_e exp (mg/g)	4.103	8.787	14.368	19.586
	q_e calc (mg/g)	1.402	2.345	4.249	5.532
	k_1 (min^{-1})	0.025	0.032	0.020	0.020
	R^2	0.581	0.587	0.823	0.944
Pseudo second order	q_e exp (mg/g)	4.103	8.787	14.368	19.586
	q_e calc (mg/g)	4.061	8.787	14.577	19.920
	k_2 (g/mg min)	0.083	0.057	0.015	0.009
	R^2	0.999	0.999	0.999	0.999

for PF-O. The main reason is probably due to the inorganic-organic adsorbent character for NiAl LDH/Biochar, biochar, and Ni/Al LDH. Furthermore, the value of k_2 for NiAl LDH/Biochar and biochar was decreased with increasing concentration of methylene blue. These phenomena are also similar for k_1 of Ni/Al LDH. The reason is that the mobility of the concentrated sample is lower than the aqueous sample. The value of k_2 is getting low for both the dyes, which indicates that the adsorption process is rapid. It means that two molecules can be adsorbed in a single site, or a single molecule can interact with two adsorption sites. Furthermore, this finding also supports that the adsorption rate depends on active sites proposing a chemisorption process.

The effect of initial concentration and temperature adsorption of methylene blue on NiAl LDH/Biochar, biochar, and Ni/Al LDH was presented in Fig. 9. The amount of methylene blue adsorbed on materials was sharply increased by increasing the initial concentration of methylene blue and temperature. The adsorption patterns for Ni/Al LDH and biochar were similar to the form two stages adsorption step. Still, NiAl LDH/Biochar has a straight adsorption pattern toward initial concentration and temperature. The isotherm Langmuir and Freundlich, as shown in Table 4 was obtained from data in Fig. 8 using the equation as following [37]:

Langmuir:

$$\frac{C}{m} = \frac{1}{bK_L} + \frac{C}{b} \quad (3)$$

where C is a saturated concentration of adsorbate; m is the amount of adsorbate; b is the maximum adsorption capacity (mg g^{-1}), and K_L is the Langmuir constant (L mg^{-1}).

Freundlich:

$$\log q_e = \log K_F + 1/n \log C_e \quad (4)$$

where q_e is adsorption capacity at equilibrium (mg g^{-1}); C_e is the adsorbate concentration at equilibrium (mg L^{-1}), and K_F is Freundlich constant. Table 4 showed the maximum adsorption capacity of Langmuir by NiAl LDH/Biochar was 61.728 mg/g, which is relatively higher than some previously reported in Table 5. Table 5 was shown the comparison of the adsorption capacity of methylene blue using several adsorbents.

The data in Table 4 showed that the adsorption of methylene blue on NiAl LDH/Biochar, biochar, and Ni/Al LDH almost follows the Langmuir isotherm adsorption model rather than the Freundlich model. The R^2 for Langmuir isotherm is nearly close to one than Freundlich isotherm. The Q_m for NiAl LDH/Biochar is higher than biochar and Ni/Al LDH. As expected of increasing surface area properties, this higher Q_m is a logical result.

The thermodynamic data, as shown in Table 6, was also calculated from data in Fig. 9 using the equation as follow:

$$\ln K_L = \frac{\Delta S}{R} - \frac{\Delta H}{RT} \quad (5)$$

$$\Delta G^\circ = -RT \ln K_L \quad (6)$$

where T is the temperature (K), R is the gas constant (8.314 J mol^{-1} K^{-1}), and K_L is the Langmuir constant from Table 4.

For all methylene blue conditions, the ΔG of

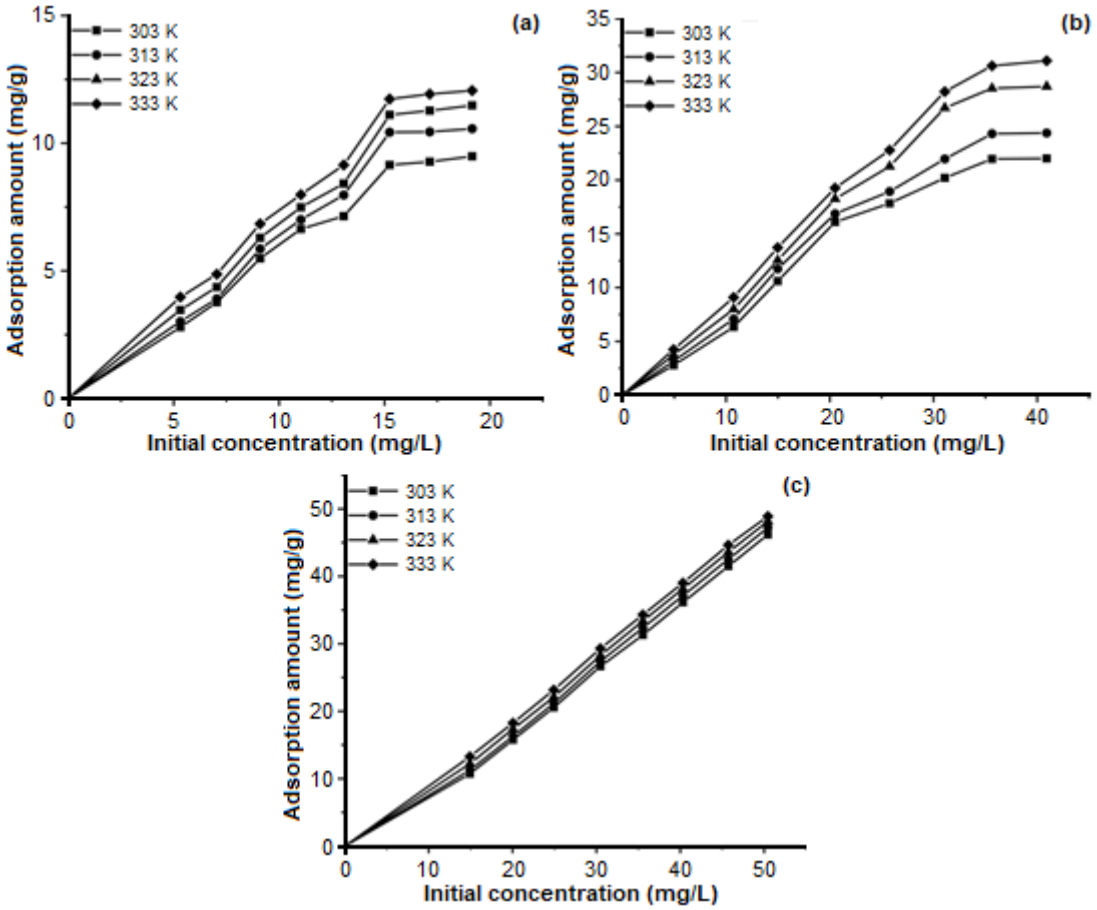

Fig 9. The effect of initial concentration and temperature adsorption on Ni/Al LDH (a), biochar (b), and NiAl LDH/Biochar (c)

Table 4. The isotherm adsorption of methylene blue

Adsorbent	Isotherm					
	Langmuir			Freundlich		
	Q_m	K_L	R^2	n	K_F	R^2
NiAl LDH	22.989	0.173	0.919	1.477	3.603	0.953
Biochar	36.101	0.622	0.990	4.296	1.336	0.993
NiAl LDH/Biochar	61.728	0.354	0.945	0.621	1.423	0.987

adsorption has a negative value means adsorption of methylene blue on NiAl LDH/Biochar, biochar, and Ni/Al LDH have spontaneously occurred in a batch small reactor system. The ΔH value is less than 80 kJ/mol and in the range 15.502–43.402 kJ/mol for all adsorbents. This value belongs to chemi-physical adsorption [51]. The value of ΔS is irregular for increasing methylene blue concentration means growing randomness for adsorption of methylene blue on the adsorbent.

Desorption of methylene blue on NiAl LDH/Biochar and starting materials were conducted using several reagents such as ethanol, acetone, diethyl ether, sodium hydroxide solution, hydrochloric acid solution, and water. The results are shown in Figure 10. NiAl LDH/Biochar and biochar were efficiently desorbed using acetone and Ni/Al LDH using hydrochloric acid. The involvement of acid-base reaction in the desorption using Ni/Al LDH was dominated,

Table 5. Comparison of the adsorption capacity of methylene blue

Adsorbent	Adsorption capacity (mg/g)	References
Wheat shells	21.50	[38]
Activated biochar-TA	53.28	[39]
MW-SiO_2	186.1	[40]
MgAl LDO	49.53	[41]
Cockle Shells-Treated Banana Pith	85.47	[42]
MgAl LDH	49	[43]
Alginate Beads Powder	48.2	[44]
Activated Carbon	11.40	[45]
Fe/SCD-LDH	83.40	[46]
Orange Peels	18.60	[10]
Rice husk	40.58	[47]
Catton Waste	24.00	[48]
Ca/Al LDH-biochar	32.535	[49]
LDH-bacteria aggregates	5.23	[50]
NiAl/Biochar	61.728	This study

Table 6. The thermodynamic parameter adsorption of methylene blue

Initial Concentration	T (K)	Q_e (mg/g)	ΔH (kJ/mol)	ΔS (J/mol K)	ΔG (kJ/mol)
NiAl LDH	303	9.489	15.502	0.051	-0.489
	313	10.570			-1.094
	323	11.479			-1.700
	333	12.061			-2.306
Biochar	303	16.097	40.951	0.145	-2.945
	313	16.873			-4.394
	323	18.255			-5.843
	333	19.269			-7.292
NiAl LDH/Biochar	303	15.661	43.402	0.153	-2.883
	313	16.533			-4.410
	323	17.878			-5.938
	333	18.924			-7.465

but like dissolve like principle [52] is found in the desorption of methylene blue on NiAl LDH/Biochar and biochar.

The regeneration of adsorbent was studied after desorption using suitable reagents as described in Fig. 10 following by washing by water several times and dried at 110 °C. It was performed until three-cycle adsorption of methylene blue using the same adsorbent from fresh materials. The results of the regeneration process are shown in Fig. 11. The reusability of Ni/Al LDH and biochar was sharply decreased for second and third cycle adsorption. At the same time, the NiAl LDH/Biochar is almost stable until the three-cycle adsorption process. The structure of Ni/Al LDH is easily exfoliated during the second and third reuse cycles. Biochar is also unstable toward reuse adsorbent due to the stability of organic materials toward washing and drying. On the other hand, NiAl LDH/Biochar has almost stable reuse adsorbent until the third cycle adsorption process due to small particle formation during NiAl LDH/Biochar synthesis as presented in SEM photos. Thus NiAl LDH/Biochar in this research is a promising adsorbent for high reusability adsorption of methylene blue.

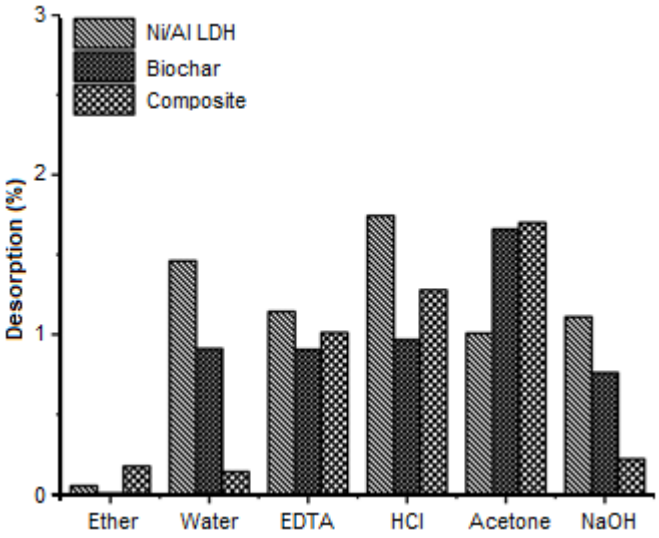

Fig 10. Desorption of methylene blue

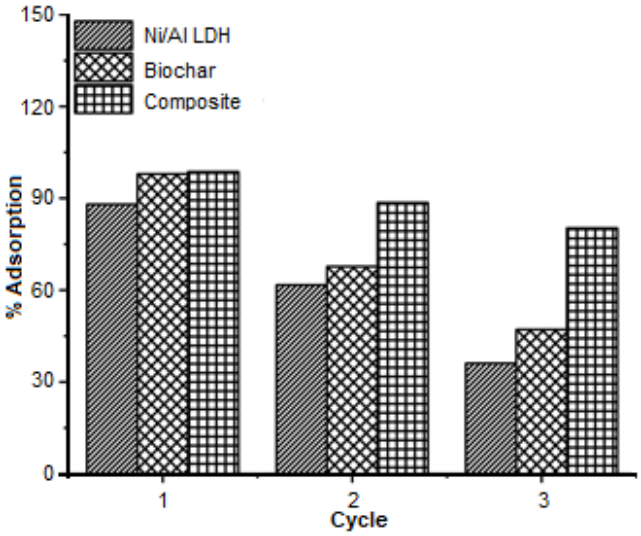

Fig 11. Cycling process of adsorbent

■ CONCLUSION

Ni/Al LDH-biochar NiAl LDH/Biochar has diffraction at 11.63° and 22.30°. NiAl LDH/Biochar has the vibration of both biochar and LDH at wavenumber 3441 cm^{-1}, 2931 cm^{-1}, 2368 cm^{-1}, 2283 cm^{-1}, 1627 cm^{-1}, 1381 cm^{-1}, 1049 cm^{-1}, and 578 cm^{-1}. NiAl LDH/Biochar has more than ten-fold surface area properties (438.942 m^2/g) than biochar (50.936 m^2/g), and Ni/Al layered double hydroxide (92.682 m^2/g). Thermal analysis showed that NiAl LDH/Biochar has one endothermic peak and two exothermic peaks related to both starting materials. NiAl LDH/Biochar has a small agglomeration and a more regular form than starting materials. Adsorption of methylene blue on NiAl LDH/Biochar follows the pseudo-second-order kinetic adsorption model and is classified as chemi-physical adsorption. NiAl LDH/Biochar has high reusability properties and can be used as a potential adsorbent to remove methylene blue from an aqueous solution.

■ ACKNOWLEDGMENTS

Authors thank Universitas Sriwijaya for this research's financial support by Hibah Profesi 2020–2021 No. 0687/UN9/SK.BUK.KP/2020 and thank Research Center of Inorganic Materials and Complexes FMIPA Universitas Sriwijaya for analysis instrumentation measurement.

■ AUTHOR CONTRIBUTIONS

NRP and RJS conducted the experiment, collecting and assembling the data; AL wrote the manuscript and concept of the research; TT and NH analysis, and interpreted the data. All authors agreed to the final version of this manuscript.

■ REFERENCES

[1] Hu, H., Wageh, S., Al-Ghamdi, A.A., Yang, S., Tian, Z., Cheng, B., and Ho, W., 2020, NiFe-LDH nanosheet/carbon fiber nanocomposite with enhanced anionic dye adsorption performance, *Appl. Surf. Sci.*, 511, 145570.

[2] Yaseen, M., Singh, M., and Ram, D., 2014, Growth, yield and economics of vetiver (*Vetiveria zizanioides* L. Nash) under intercropping system, *Ind. Crops Prod.*, 61, 417–421.

[3] Tezcan Un, U., and Ates, F., 2019, Low-cost adsorbent prepared from poplar sawdust for removal of disperse orange 30 dye from aqueous solutions, *Int. J. Environ. Sci. Technol.*, 16 (2), 899–908.

[4] Palapa, N.R., Juleanti, N., Taher, T., and Lesbani, A., 2020, Unique adsorption properties of malachite green on interlayer space of Cu-Al and Cu-Al-$SiW_{12}O_{40}$ layered double hydroxides, *Bull. Chem. React. Eng. Catal.*, 15 (3), 653–661.

[5] Yan, H., Li, H., Yang, H., Li, A., and Cheng, R., 2013, Removal of various cationic dyes from aqueous solutions using a kind of fully biodegradable magnetic composite microsphere, *Chem. Eng. J.*, 223, 402–411.

[6] Long, Y., Wang, Y., Zhang, D., Ju, P., and Sun, Y., 2016, Facile synthesis of BiOI in hierarchical nanostructure preparation and its photocatalytic application to organic dye removal and biocidal effect of bacteria, *J. Colloid Interface Sci.*, 481, 47–56.

[7] Soleimani, K., Tehrani, A.D., and Adeli, M., 2018, Bioconjugated graphene oxide hydrogel as an effective adsorbent for cationic dyes removal, *Ecotoxicol. Environ. Saf.*, 147, 34–42.

[8] Logita, H.H., Tadesse, A., and Kebede, T., 2015, Synthesis, characterization and photocatalytic activity of $MnO_2/Al_2O_3/Fe_2O_3$ nanocomposite for degradation of malachite green, *Afr. J. Pure Appl. Chem.*, 9 (11), 211–222.

[9] Meili, L., Lins, P.V., Zanta, C.L.P.S., Soletti, J.I., Ribeiro, L.M.O., Dornelas, C.B., Silva, T.L., and Vieira, M.G.A., 2019, MgAl-LDH/Biochar composites for methylene blue removal by adsorption, *Appl. Clay Sci.*, 168, 11–20.

[10] Annadurai, G., Juang, R.S., and Lee, D.J., 2002, Use of cellulose-based wastes for adsorption of dyes from aqueous solutions, *J. Hazard. Mater.*, 92 (3), 263–274.

[11] Elmoubarki, R., Mahjoubi, F.Z., Elhalil, A., Tounsadi, H., Abdennouri, M., Sadiq, M., Qourzal, S., Zouhri, A., and Barka, N., 2017, Ni/Fe and Mg/Fe layered double hydroxides and their calcined derivatives: Preparation, characterization and application on textile dyes removal, *J. Mater. Res. Technol.*, 6 (3), 271–283.

[12] Özdemir, M., Durmuş, Ö., Şahin, Ö., and Saka, C., 2016, Removal of methylene blue, methyl violet, rhodamine B, alizarin red, and bromocresol green dyes from aqueous solutions on activated cotton stalks, *Desalin. Water Treat.*, 57 (38), 18038–18048.

[13] Zhang, P., O'Connor, D., Wang, Y., Jiang, L., Xia, T., Wang, L., Tsang, D.C.W., Ok, Y.S., and Hou, D., 2020, A green biochar/iron oxide composite for methylene blue removal, *J. Hazard. Mater.*, 384, 121286.

[14] Kubo, D., Tadanaga, K., Hayashi, A., and Tatsumisago, M., 2012, Hydroxide ion conduction in Ni-Al layered double hydroxide, *J. Electroanal. Chem.*, 671, 102–105.

[15] Oktrianti, M., Palapa, N.R., Mohadi, R., and Lesbani, A., 2020, Effective removal of iron(II) from aqueous solution by adsorption using Zn/Cr layered double hydroxides intercalated with Keggin ion, *J. Ecol. Eng.*, 21 (5), 63–71.

[16] Liao, X.J., and Chen, G.S., 2016, A hybrid hydrogel based on clay nanoplatelets and host-guest inclusion complexes, *Chin. Chem. Lett.*, 27 (4), 583–587.

[17] González, M.A., Pavlovic, I., and Barriga, C., 2015, Cu(II), Pb(II) and Cd(II) sorption on different layered double hydroxides. A kinetic and thermodynamic study and competing factors, *Chem. Eng. J.*, 269, 221–228.

[18] Guo, Y., Zhu, Z., Qiu, Y., and Zhao, J., 2013, Synthesis of mesoporous Cu/Mg/Fe layered double hydroxide and its adsorption performance for arsenate in aqueous solutions, *J. Environ. Sci.*, 25 (5), 944–953.

[19] Kovanda, F., Jindová, E., Lang, K., Kubát, P., and Sedláková, Z., 2010, Preparation of layered double hydroxides intercalated with organic anions and their application in LDH/poly(butyl methacrylate) nanocomposites, *Appl. Clay Sci.*, 48 (1-2), 260–270.

[20] Liu, Z., and Zhang, F.S., 2009, Removal of lead from water using biochars prepared from hydrothermal liquefaction of biomass, *J. Hazard. Mater.*, 167 (1-3), 933–939.

[21] Tan, X., Liu, Y., Zeng, G., Wang, X., Hu, X., Gu, Y., and Yang, Z., 2015, Application of biochar for the removal of pollutants from aqueous solutions, *Chemosphere*, 125, 70–85.

[22] Ahmad, R., and Mondal, P.K., 2010, Application of modified water nut carbon as a sorbent in Congo red and Malachite green dye contaminated wastewater remediation, *Sep. Sci. Technol.*, 45 (3), 394–403.

[23] Wan, S., Wang, S., Li, Y., and Gao, B., 2017, Functionalizing biochar with Mg–Al and Mg–Fe layered double hydroxides for removal of

phosphate from aqueous solutions, *J. Ind. Eng. Chem.*, 47, 246–253.

[24] Zhang, M., Gao, B., Yao, Y., and Inyang, M., 2013, Phosphate removal ability of biochar/MgAl-LDH ultra-fine composites prepared by liquid-phase deposition, *Chemosphere*, 92 (8), 1042–1047.

[25] Zubair, M., Manzar, M.S., Mu'azu, N.D., Anil, I., Blaisi, N.I., and Al-Harthi, M.A., 2020, Functionalized MgAl-layered hydroxide intercalated date-palm biochar for enhanced uptake of cationic dye: Kinetics, isotherm and thermodynamic studies, *Appl. Clay Sci.*, 190, 105587.

[26] Lins, P.V.S., Henrique, D.C., Ide, A.H., da silva Duarte, J.L., Dotto, G.L., Yazidi, A., Sellaoui, L., Erto, A., Zanta, C.L.P.S., and Meili, L., 2020, Adsorption of a non-steroidal anti-inflammatory drug onto MgAl/LDH-activated carbon composite – Experimental investigation and statistical physics modeling, *Colloids Surf., A*, 586, 124217.

[27] Wang, S., Gao, B., Li, Y., Zimmerman, A.R., and Cao, X., 2016, Sorption of arsenic onto Ni/Fe layered double hydroxide (LDH)-biochar composites, *RSC Adv.*, 6 (22), 17792–17799.

[28] Palapa, N.R., Mohadi, R., and Lesbani, A., 2018, Adsorption of direct yellow dye from aqueous solution by Ni/Al and Zn/Al layered double hydroxides, *AIP Conf. Proc.*, 2026, 020018.

[29] Bai, Z., Hu, C., Liu, H., and Qu, J., 2019, Selective adsorption of fluoride from drinking water using NiAl-layered metal oxide film electrode, *J. Colloid Interface Sci.*, 539, 146–151.

[30] Tao, X., Han, Y., Sun, C., Huang, L., and Xu, D., 2019, Plasma modification of NiAlCe–LDH as improved photocatalyst for organic dye wastewater degradation, *Appl. Clay Sci.*, 172, 75–79.

[31] Xiao, F., Cheng, J., Cao, W., Yang, C., Chen, J., and Luo, Z., 2019, Removal of heavy metals from aqueous solution using chitosan-combined magnetic biochars, *J. Colloid Interface Sci.*, 540, 579–584.

[32] Xia, Y., Yang, T., Zhu, N., Li, D., Chen, Z., Lang, Q., Liu, Z., and Jiao, W., 2019, Enhanced adsorption of Pb(II) onto modified hydrochar: Modeling and mechanism analysis, *Bioresour. Technol.*, 288, 121593.

[33] Wang, T., Li, C., Wang, C., and Wang, H., 2018, Biochar/MnAl-LDH composites for Cu(II) removal from aqueous solution, *Colloids Surf., A*, 538, 443–450.

[34] Shaji, A., and Zachariah, A.K., 2017, "Surface area analysis of nanomaterials, in *Micro and Nano Technologies, Thermal and Rheological Measurement Techniques for Nanomaterials Characterization*, Volume 3, Eds. Thomas, S., Thomas, R., Zachariah, A.K., and Mishra, R.K., Elsevier Inc., 197–231.

[35] Beakou, B.H., El Hassani, K., Houssaini, M.A., Belbahloul, M., Oukani, E., and Anouar, A., 2017, A novel biochar from *Manihot esculenta* Crantz waste: Application for the removal of malachite green from wastewater and optimization of the adsorption process, *Water Sci. Technol.*, 76 (6), 1447–1456.

[36] Iftekhar, S., Ramasamy, D.L., Srivastava, V., Asif, M.B., and Sillanpää, M., 2018, Understanding the factors affecting the adsorption of Lanthanum using different adsorbents: A critical review, *Chemosphere*, 204, 413–430.

[37] Kushwaha, A.K., Gupta, N., and Chattopadhyaya, M.C., 2014, Removal of cationic methylene blue and malachite green dyes from aqueous solution by waste materials of *Daucus carota*, *J. Saudi Chem. Soc.*, 18 (3), 200–207.

[38] Bulut, E., Özacar, M., and Şengil, İ.A., 2008, Adsorption of malachite green onto bentonite: Equilibrium and kinetic studies and process design, *Microporous Mesoporous Mater.*, 115 (3), 234–246.

[39] Wang, Y., Zhang, Y., Li, S., Zhong, W., and Wei, W., 2018, Enhanced methylene blue adsorption onto activated reed-derived biochar by tannic acid, *J. Mol. Liq.*, 268, 658–666.

[40] Peres, E.C., Slaviero, J.C., Cunha, A.M., Hosseini–Bandegharaei, A., and Dotto, G.L., 2018, Microwave synthesis of silica nanoparticles and its application for methylene blue adsorption, *J. Environ. Chem. Eng.*, 6 (1), 649–659.

[41] Qiao, Y., Li, Q., Chi, H., Li, M., Lv, Y., Feng, S., Zhu, R., and Li, K., 2018, Methyl blue adsorption properties and bacteriostatic activities of Mg-Al layer oxides via a facile preparation method, *Appl. Clay Sci.*, 163, 119–128.

[42] Hasan, R., Ying, W.J., Cheng, C.C., Jaafar, N.F., Jusoh, R., Jalil, A.A., and Setiabudi, H.D., 2020, Methylene blue adsorption onto cockle shells-treated banana pith: Optimization, isotherm, kinetic, and thermodynamic studies, *Indones. J. Chem.*, 20 (2), 368–378.

[43] Aguiar, J.E., Bezerra, B.T.C., Braga, B.M., Lima, D.S., Nogueira, R.E.F.Q., de Lucena, S.M.P., and da Silva, I.J., 2013, Adsorption of anionic and cationic dyes from aqueous solution on non-calcined Mg-Al layered double hydroxide: Experimental and theoretical study, *Sep. Sci. Technol.*, 48 (15), 2307–2316.

[44] Purnaningtyas, M.A.K., Sudiono, S., and Siswanta, D., 2020, Synthesis of activated carbon/chitosan/alginate beads powder as an adsorbent for methylene blue and methyl violet 2B dyes, *Indones. J. Chem.*, 20 (5), 1119–1130.

[45] Rao, V.V.B., and Rao, S.R.M., 2006, Adsorption studies on treatment of textile dyeing industrial effluent by fly ash, *Chem. Eng. J.*, 116 (1), 77–84.

[46] Hu, W., Wu, X., Jiao, F., Yang, W., and Zhou, Y., 2016, Preparation and characterization of magnetic Fe_3O_4@sulfonated β-cyclodextrin intercalated layered double hydroxides for methylene blue removal, *Desalin. Water Treat.*, 57 (53), 25830–25841.

[47] Vadivelan, V., and Kumar, K.V., 2005, Equilibrium, kinetics, mechanism, and process design for the sorption of methylene blue onto rice husk, *J. Colloid Interface Sci.*, 286 (1), 90–100.

[48] Yavuz, E., Bayramoğlu, G., Arica, M.Y., and Senkal, B.F., 2011, Preparation of poly (acrylic acid) containing core-shell type resin for removal of basic dyes, *J. Chem. Technol. Biotechnol.*, 86 (5), 699–705.

[49] Lesbani, A., Asri, F., Palapa, N.R., Taher, T., and Rachmat, A., 2020, Efficient removal of methylene blue by adsorption using composite based Ca/Al layered double hydroxide-biochar, *Global NEST J.*, 22 (2), 250–257.

[50] Liu, J., Li, X., Luo, J., Duan, C., Hu, H., and Qian, G., 2014, Enhanced decolourisation of methylene blue by LDH-bacteria aggregates with bioregeneration, *Chem. Eng. J.*, 242, 187–194.

[51] Taher, T., Mohadi, R., Rohendi, D., and Lesbani, A., 2017, Kinetic and thermodynamic adsorption studies of Congo red on bentonite, *AIP Conf. Proc.*, 1823, 020028.

[52] Mahmoodi, N.M., Hayati, B., Arami, M., and Lan, C., 2011, Adsorption of textile dyes on Pine Cone from colored wastewater: Kinetic, equilibrium and thermodynamic studies, *Desalination*, 268 (1-3), 117–125.